THE JOURNAL OF PHYSICAL CHEMISTRY B

ARTICLE

pubs.acs.org/JPCB

Pressure-Induced Fluorescence of Pyridine

Samuele Fanetti,[†] Margherita Citroni,[*,†] and Roberto Bini[†,‡]

[†]LENS - European Laboratory for Nonlinear Spectroscopy, Università di Firenze, via N. Carrara 1, I-50019 Sesto F.no (FI), Italy

[‡]Dipartimento di Chimica dell' Università di Firenze, via della Lastruccia 3, I-50019 Sesto F.no (FI), Italy

ABSTRACT: Two-photon excitation profiles and fluorescence spectra have been measured as a function of pressure in a diamond anvil cell up to 15.5 GPa in crystal phases I and II and in the glassy form of pyridine. The fluorescence emission intensity increases by about 6 orders of magnitude in going from the liquid to the crystalline phases at 3 GPa and further increases with pressure. This is explained by an energy inversion of the lowest $^1B_1$ ($n\pi^*$) and $^1B_2$ ($\pi\pi^*$) excited states likely due to the involvement of the lone pair of the N atom in intermolecular CH···N bonds. These interactions characterize the crystal phases and are stabilized by pressure. The glassy form, accordingly, is characterized by a much weaker fluorescence. Excimer emission is also observed. Comparison of the emission of several samples with different compression and annealing histories, the lack of reversibility in the excimer emission with decompression, and the larger relative intensity of the excimer band in the glassy form suggest that excimer formation occurs at crystal defects. This results support the conclusions of a previous investigation proposing that pressure-induced reactivity of pyridine is limited to crystal defects and agrees with the present knowledge of the solid-state chemistry of aromatic crystals.

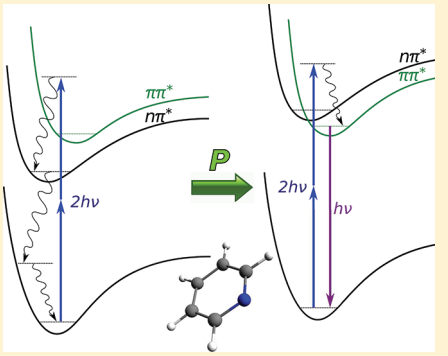

1. INTRODUCTION

The photophysical and photochemical properties of pyridine are of great interest due to the relatively simple and paradigmatic structure of this molecule. Pyridine, a prototype of heteroaromatics, is also an interesting case study in the field of pressure-induced reactivity in the solid state. Chemical reactivity at very high pressures,[1] particularly in unsaturated molecular systems, is an appealing field of investigation both from a fundamental point of view and because of its promising applications for eco-friendly synthetic methods. The low-lying electronic excited states play a key role in the high-pressure reactivity of molecular systems. In particular, selective electronic excitation through two-photon (TP) absorption of laser light has been successfully used in conjunction with high pressure to obtain selective polymerizations,[2,3] to remarkably lower the reaction threshold pressure in several unsaturated molecular systems,[4] and to trigger chemical reactions in otherwise stable systems at high pressure, as in the production of molecular hydrogen from N_2—water mixtures.[5] Investigation of the electronic structure of the reacting systems near the reaction threshold pressure then turns out to be of great importance in understading the mechanisms of pressure-induced reactivity. This has been long recognized, particularly by Drickamer and co-workers, which dedicated a great part of their work to elucidate the behavior of electronic states under pressure[6] and their implications in solid-state chemistry.[7] In particular they showed how the different response of the molecular orbitals to the increased density causes relative shifts in the energies of the electronic states. The pressure tuning of the emission properties of aromatic molecules in solid matrices or in their crystals phases is up to now an attractive research topic.[8,9]

The high-pressure spectroscopic investigation of small model molecules, a starting point to understand reactivity in the condensed phases, deserves some comment regarding the experimental conditions required. The diamond absorption edge, located around 250 nm, limits the wavelength range that can be used in optical spectroscopy measurements, so that for most investigated systems, whose lowest excited states fall in the UV range, the exploitation of TP absorption techniques is needed. The typically small TP absorption cross sections make a direct measurement of TP absorption not possible in a diamond anvil cell (DAC). Indirect detection methods are required, the most used being the detection of TP induced fluorescence. On the other hand, the small TP absorption cross sections determine the presence of a very small amount of excited molecules in the sample, allowing a better control in the photochemical activation procedures and making these spectroscopic studies a valid support to understand the high-pressure photoinduced reactive processes.

The relation between the pressure-induced reactivity, the crystal structure, and the pressure evolution of the electronic states has been evidenced through the measurement of fluorescence spectra and TP excitation profiles for benzene[10] and indole.[11] The high-pressure chemistry and photochemistry of aromatic systems deserves a particular attention for its potential in the synthesis of valuable amorphous hydrogenated materials with appealing technological properties.[12] The high-pressure reactivity of benzene represents a benchmark for understanding the high-pressure chemical behavior of aromatics both from a theoretical[13] and an

Received: July 19, 2011
Revised: September 8, 2011
Published: September 21, 2011

experimental point of view.[14] The characterization of the reactivity in different pressure−temperature conditions in conjunction with ab initio calculations have evidenced the involvement, in the reaction onset, of dimeric configurations forming in the high-pressure crystal phase II[14] and matching the geometry of excimers that form upon excitation to the low-lying electronic states.[10] On the contrary, the crystal structure of indole does not allow excimer formation, and this results in a great chemical and photochemical stability at least up to 25 GPa.[11] In this case, both excimer formation and reaction nucleation are only possible at the structural defects of the crystal.

Pyridine is characterized by a rich polymorphism at high pressure.[15] Room-temperature studies have evidenced two orthorhombic crystal phases (I and II) and a glassy form. Both crystal phase I[16] and II[17] have been resolved. Transitions among these phases are kinetically driven, and the stability and metastability ranges and the pressure−temperature cycles necessary to achieve them have been recently reported.[15] Similarly to benzene,[14] which chemically transforms into an amorphous hydrogenated carbon above 40 GPa in annealed samples and above 23 GPa in not-annealed samples, and to furan[18] and thiophene,[19] which undergo similar transformations, pyridine also reacts at room temperature above 18 GPa giving rise to an amorphous solid.[15,20] Also, similarly to benzene[21] and furan,[22] the reaction threshold pressure of pyridine is lowered by about a factor of 3 by TP absorption of visible light at 457 nm.[15] Nevertheless, in the case of pyridine the limited extent of the transformation and its reduction with increasing the crystal quality suggested a defect-driven reactivity.[15]

Experimental characterization of the lowest excited states of pyridine as a function of pressure is of primary importance in elucidating the mechanism through which the threshold pressure for the formation of the reaction seeds is strongly lowered by photoactivation. In crystalline phase II of benzene the formation of excimers through TP excitation to the lowest excited states at sufficiently high pressure has been shown to be related to the onset of the pressure induced reactivity, whereas in indole the crystal packing, which prevents excimer formation, is also responsible for chemical stability at high pressure. The present study is therefore aimed to evidence the connection among electronic and structural properties and pressure-induced reactivity. However, like most molecular systems where the lowest excited state is of $n\pi^*$ character, pyridine has an extremely weak fluorescence, which has only been observed in the vapor phase at low pressures.[23] A TP spectrum of liquid pyridine has been obtained at ambient conditions by the thermal-lensing technique,[24] while no data are available on electronic excited states of pyridine in its solid phases.

In the present work, we have observed a TP-induced fluorescence strongly intensifying upon increasing pressure, indicating that the density increase remarkably affects the electronic structure of the system. The fluorescence spectra and the TP excitation profiles have been investigated at room temperature in the three solid polymorphs below the threshold of the pressure-induced reaction. Interpretation of the results yields a consistent view of the role of the low-lying excited states and of the crystal structure in the high-pressure reactivity.

2. EXPERIMENTAL METHODS

High pressure was generated in a membrane diamond anvil cell (MDAC) equipped with IIa type diamonds selected for low fluorescence. Pyridine (Aldrich, 99.9%) was distilled in N_2 stream over KOH to eliminate residual water and kept in a bottle with KOH to avoid water contamination. Rhenium gaskets with initial sample dimensions of about 50 μm in thickness and 150 μm in diameter were used. TP excitation profiles and fluorescence spectra were measured by using as excitation source an optical parametric generator (EKSPLA - PG401) pumped by the third harmonic (355 nm) of a mode-locked Nd:YAG laser (EKSPLA - PL2143A) with a pulse duration of about 20 ps and a repetition rate of 10 Hz. The beam was attenuated by reflection on BK7 beamsplitters and by neutral density filters, to have a maximum incident energy per pulse of about 1 μJ on the DAC, and was focused on the sample by an achromatic doublet with a focal length of 100 mm. Before focalization, about 3% of the beam energy was reflected onto a fast UV-enhanced Si photodiode (Hamamatsu, S1722−02) for signal normalization. Emission from the sample was collected in backscattering geometry through a parabolic mirror and analyzed by a single stage $^1/_4$ m monochromator (2400 grooves per mm) coupled to a photomultiplier tube (ET-9235QB). A UG11 filter was used to cut the excitation beam reflected by the diamond anvils. The fluorescence spectra were obtained with a monochromator resolution of about 1 nm. The spectral sampling of the excitation profiles, determined by the amplitude of the tuning steps of the PG, was set to 1 nm because the spectra did not reveal narrower lines at higher resolution. For the measurement of the excitation profiles the fluorescence was collected around its maximum with a monochromator bandpass of about 10 nm. An oscilloscope (LeCroy LC584A) was used to collect the signals from the PMT and from the reference photodiode. For each data point, both signals were averaged over 150 laser pulses, and the average integrated areas and amplitudes were recorded. Normalization of the fluorescence signal on the incident pulse intensity was performed according to a quadratic dependence, which was checked before and after each measured spectrum at several excitation wavelengths. Because of the low fluorescence quantum yield of pyridine at the lower pressures, alignment of the optical setup was achieved using a similar MDAC containing crystalline benzene, which has a rather high fluorescence signal in similar TP excitation and detection conditions.[10]

No pressure calibrants were used, to avoid interferences with the processes under examination and with the pyridine signal due to any thermal, photochemical, or photophysical effects of the calibrant itself. The pressure was estimated by measuring the FTIR spectrum before and after any excitation or emission spectrum and comparing the absorption frequencies with those measured in IR experiments where the ruby fluorescence method was used for pressure calibration. In particular, the pressure dependence of the Davydov components of the mixed ν_3 and ν_{9a} modes (in Wilson's notation) was used. A large amount of vibrational data were available, on samples having different compression and annealing histories and in different solid forms. The uncertainty in the pressure evaluation is estimated to be about ±0.2 GPa. The measurement of the IR spectrum was also essential to determine whether the sample was in the liquid phase, in the crystalline phase I or II, or in the glassy form[15] and to detect any sign of the onset of a chemical reaction. The IR spectra were recorded in the mid-IR region 600−5000 cm^{-1} with a spectral resolution of 1 cm^{-1}, using a Bruker IFS-120HR FTIR spectrometer especially modified to allow measurements in the MDAC with a remote control and in situ measurement of pressure.[25]

3. RESULTS

As a preliminary step we have tried to measure a fluorescence spectrum of liquid pyridine at ambient conditions in a 10 mm thick quartz cuvette. A weak fluorescence signal, just above our

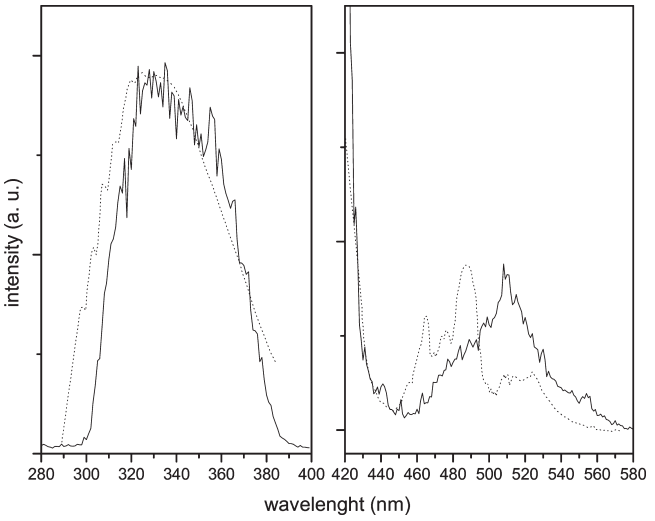

Figure 1. Left panel: fluorescence spectrum of liquid pyridine at room conditions measured in a quartz cuvette, with TP excitation at 485 nm (solid line), compared to the fluorescence spectrum of pyridine vapor at 20 Torr with one-photon excitation at 287.5 nm (dotted line).[26] Right panel: TP excitation profile of liquid pyridine at room conditions in a quartz cuvette (solid line), compared to the TP absorption spectrum of liquid pyridine measured by the thermal lensing technique.[24] The spectra have been multiplied by arbitrary factors to obtain similar intensities.

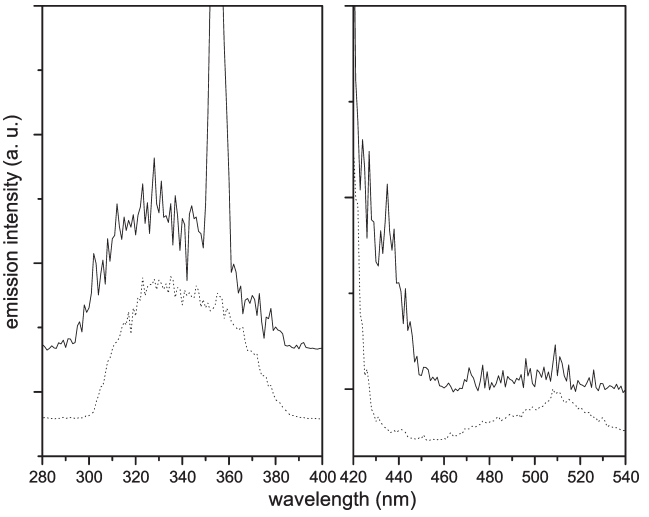

Figure 2. Left panel: fluorescence spectrum of pyridine in crystal phase II at 3.1 GPa (solid line) and in the liquid phase in the cuvette (dashed line), obtained through TP excitation at 436 and 485 nm, respectively. The band at 355 nm is due to scattered light from the pump laser entering the monochromator. Right panel: TP excitation profile of pyridine in crystal phase II at 3.1 GPa (solid line) and in the liquid phase in the cuvette (dashed line). The spectra have been multiplied by arbitrary factors to obtain similar intensities.

detection threshold, was detected using an incident beam energy of about 30 μJ/pulse. The fluorescence spectrum obtained with excitation at 485 nm is shown in Figure 1, compared to the fluorescence spectrum of pyridine vapor.[26] A fluorescence spectrum of liquid pyridine is not available in the literature, to our knowledge. The spectrum as a whole is slightly red-shifted with respect to that of the vapor phase. Moreover, the intensity distribution is quite different because, besides the presence of a spurious signal due to scattered light of the pump beam at 355 nm, the red part of the liquid-phase spectrum is more intense than in the vapor phase. The fluorescence spectrum is independent of the excitation wavelength in the 420−540 nm range. The TP excitation profile that we measured on liquid pyridine is shown in the right panel of Figure 1, compared to the TP absorption spectrum of liquid pyridine obtained by thermal-lensing measurements.[24] Our data are in substantial agreement with the thermal-lensing measurement concerning the excitation frequencies. The relative intensities of the S_2 (250−270 nm) and S_3 (230−250 nm) states are inverted in the two experiments likely due to the intrinsic differences concerning the absorption determination on which the two techniques are based. A quite lower fluorescence is detected following excitation to S_3 than following excitation to S_2. The $S_0 \rightarrow S_1$ transition, whose electronic origin is located at 287.6 nm, is not observed, in agreement with the thermal lensing experiment and with the weak expected absorption cross section.[24]

No fluorescence was detected following TP excitation of liquid pyridine in the DAC at any wavelength between 420 and 600 nm. Indeed, the experimental conditions for the fluorescence excitation and detection are quite different for samples in the DAC and in the cuvette. Taking into account the quadratic dependence of the fluorescence signal upon the excitation beam intensity, the different pulse energy used in the two experiments (30 μJ/pulse on the cuvette and 0.5−1 μJ/pulse on the DAC to avoid diamond damage), and the different active path length, the detection threshold is about 5 orders of magnitude larger for samples in the DAC.

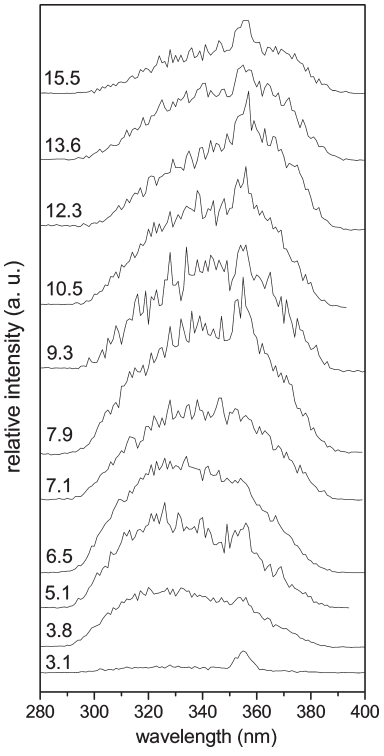

Figure 3. Emission spectra measured after TP excitation at 436 nm on pyridine in crystal phase II at different pressures, indicated in the figure in GPa units. The intensities have not been rescaled. The band at 355 nm is due to scattered light from the pump laser entering the monochromator.

The pressure was then raised very slowly, keeping the DAC aligned in the measurement position and scanning the monochromator wavelength in the 300−380 nm range, while exciting

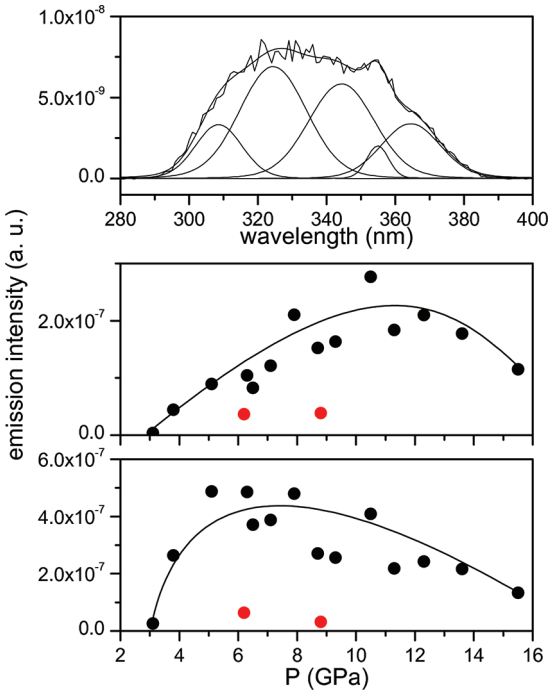

Figure 4. Top panel: decomposition of the emission spectrum measured at 6.5 GPa in the not-annealed phase II. The band at 355 nm is due to scattered light from the pump laser entering the monochromator. Middle panel: integrated area of the lowest frequency emission peak as a function of pressure. Bottom panel: sum of the integrated areas of the three high frequency emission peaks as a function of pressure. Black symbols: data from the experiment on the not-annealed crystal phase II upon compression. Red symbols: data from the experiment on the glassy form. Lines are intended as a guide for the eye.

in the 420−440 nm range and around 520 nm, until a weak emission, peaked around 330 nm, was detected. The TP excitation profile and the emission spectrum obtained through TP excitation at 436 nm are shown in Figure 2. Measurement of the FTIR spectrum and comparison with previously obtained data[15] revealed that the sample was in the crystal phase II at a pressure of 3.1 GPa. The excitation profile is quite different in these conditions with respect to the liquid: the bands assigned to the $S_0 \rightarrow S_2$ and $S_0 \rightarrow S_3$ transitions are barely detectable, while the edge of the $S_0 \rightarrow S_4$ transition is strongly red-shifted, showing some structure with a quite narrow peak around 435 nm. The fluorescence spectrum is blue-shifted with respect to the spectrum of the liquid phase, being more similar to the spectrum of the vapor phase.

The pressure was then raised in steps of about 1 GPa, at each step measuring the TP excitation profiles, the fluorescence spectrum, and the FTIR spectrum to determine the pressure. Selected emission spectra measured TP exciting the sample at 436 nm upon compression of not annealed phase II are shown in Figure 3. A sudden intensification of the fluorescence spectrum is observed between 3.1 and 3.8 GPa. The overall intensity slightly further increases up to about 8 GPa, whereas above this pressure it decreases again. It can also be noted that the relative intensity of the red part of the spectrum increases with pressure up to the highest pressure reached (15.5 GPa).

The fluorescence spectra were reproduced by a fitting program[27] using the minimum number of bands having Voigt profiles. Four peaks, plus an additional band that reproduces the residual 355 nm light entering the monochromator, were necessary for all the pressures probed, as shown in the upper panel of Figure 4 for one of the measured spectra. During the fitting procedure, the band widths were fixed, when necessary, to have consistent values all over the data set. The two central bands always had a similar width, while the highest frequency band was always slightly narrower, and the low frequency one was slightly larger, and its bandwidth increased with compression. The resulting errors on wavelengths are always below 2 nm, while the error in the integrated areas was smaller than 0.5%. Inspection of the pressure evolution of the integrated areas reveals that the three high-frequency bands have a similar behavior, increasing in intensity up to about 6 GPa and decreasing at higher pressures, while the intensity of the lowest frequency band has a different pressure dependence with a maximum at 11−12 GPa (see Figure 4). This band is red-shifted by about 5000 cm^{-1} with respect to the highest frequency band. As will be discused in the next section, several examples of emission from excimers forming in the crystal phases of aromatic systems are reported in the literature,[10,28−32] displaced by about this frequency value with respect to the exciton band. Therefore, we can confidently assign the low frequency emission band to excimeric structures forming in the crystal. The relative area of this low frequency peak resulting from our data analysis (area of the excimer band divided by the total area of the emission spectrum) is reported in Figure 5 as a function of pressure, along with the peak frequencies of the four bands. The peak frequencies of the high frequency peaks undergo a slight red shift with increasing pressure, while the frequency of the excimer band is approximately constant in the investigated pressure range. The data shown in Figure 5 result from fluorescence spectra of different samples having different compression and annealing histories, as described in the following. These measuremens were performed with the aim of elucidating the role of structural defects and strains on the intensity and spectral features of the emission spectrum. In particular, besides phase II crystals compressed without any thermal annealing, we have also investigated annealed phase II, phase I, and glassy samples, and reversibility was checked in both crystal phases I and II.

On a fresh sample, a thermal annealing at 190 °C was performed after crystallization into phase II at about 2 GPa. Fluorescence spectra were measured in the annealed phase II at 5.4 and 8.2 GPa upon compression and at 7.2, 5.4, and at 4.5 GPa upon decompression. Frequencies and bandwidhts are similar to those of the experiment on not-annealed phase II and are reversible with pressure. On the contrary, the relative intensity of the excimer peak (Figure 5) undergoes the same intensification with pressure as in the not annealed sample, but upon decompression its intensity is not reversible and remains at a quite large value in the last step of decompression.

In another sample the glassy form of pyridine was obtained,[15] and as previously done for the not-annealed phase II, it was slowly pressurized until a fluorescence signal was detected. The emission signal appeared at about 6 GPa, a quite higher pressure than in crystal phase II. The fluorescence spectrum of the glassy form was measured at 6.2 and 8.7 GPa. The overall fluorescence spectrum is much weaker than in phase II, but the relative intensity in the excimer band is a much larger, as shown in Figures 5 and 6.

Phase I was obtained upon decompression of the glassy form at 0.6 GPa. Good quality crystals were grown at the melting pressure. Fluorescence spectra were measured at 4.1 and 8.6 GPa on compression and at 3.8 GPa on decompression. As the pressure was increased without annealing, this sample contained growing quantities of phase II crystallites, resulting in an

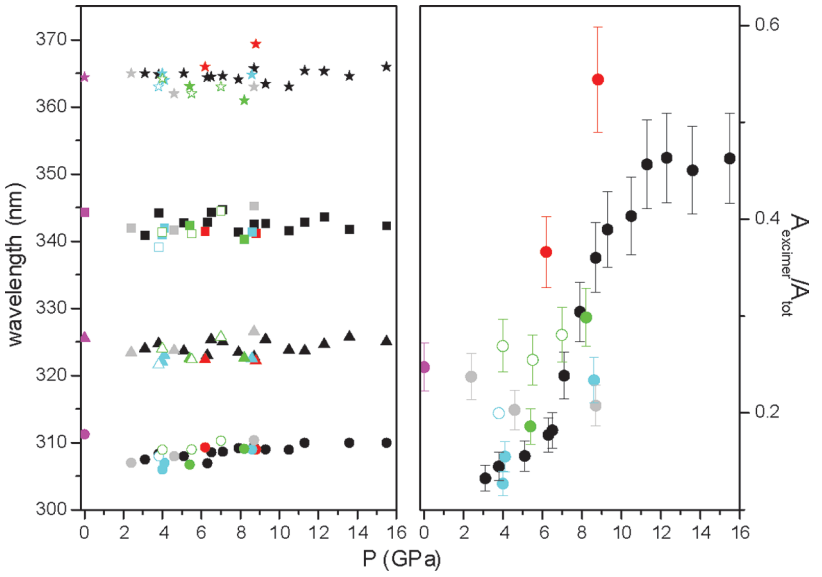

Figure 5. Results of the deconvolution of the emission spectra measured as a function of pressure. Left panel: peak frequencies. Right panel: ratio of the area of the lowest frequency peak to the total area of the emission spectrum. Magenta symbols at room pressure: liquid sample in the cuvette. Black symbols: crystal phase II upon compression, not annealed sample. Green full symbols: crystal phase II upon compression, annealed sample. Green empty symbols: crystal phase II upon decompression, annealed sample. Gray symbols: crystal phase II upon compression from phase I. Cyan full symbols: crystal phase I upon compression. Cyan empty symbols: crystal phase I upon decompression. Red symbols: glassy form upon compression.

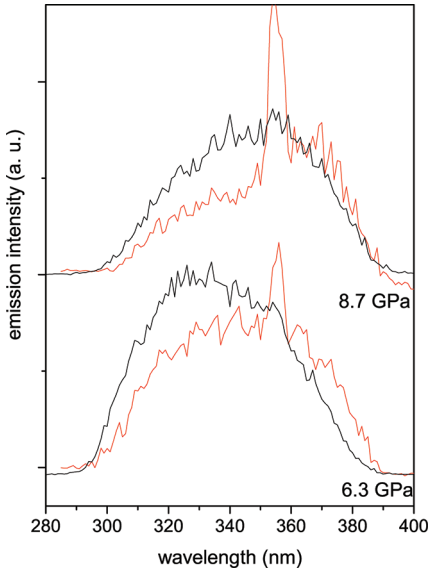

Figure 6. Emission spectra of the not-annealed phase II (black traces) and of the glassy form (red traces) at 6.3 and 8.7 GPa upon compression. The spectra of the glassy form have been multiplied by a factor 5.

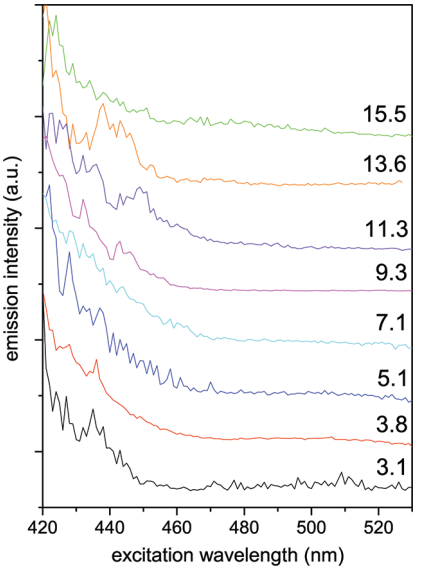

Figure 7. TP excitation profiles of pyridine in crystal phase II, measured at different pressures (GPa) as indicated in the figure. Intensity have been rescaled using the area values obtained from the fit of the fluorescence spectrum.

extremely defected mixture of the two phases. Finally, this sample was annealed, after decompression, at 2.4 GPa and a highly polycrystalline phase II was obtained, in which fluorescence spectra were measured at 2.4, 4.6, and 8.7 GPa upon compression. All these spectra have similar properties as those of the not-annealed phase II concerning the absolute intensities and the relative intensity of the excimer band, which anyway is not reversible with decompression.

A selection of TP excitation profiles measured on the not-annealed phase II as a function of pressure up to 15.5 GPa is reported in Figure 7. The onset of the $S_0 \rightarrow S_4$ transition is located at about 450 nm, a lower energy than in the liquid phase, and it does not appreciably shift as a function of pressure. The lower energy transitions are too weak to be accurately detected in our experimental conditions. TP excitation profiles measured on the other samples show no significant differences.

4. DISCUSSION

In this work we have been able to detect a fluorescence emission from solid pyridine, sharply intensifying with pressure between 3 and 4 GPa and further slightly increasing up to about

dx.doi.org/10.1021/jp2068864 |J. Phys. Chem. B 2011, 115, 12051–12058

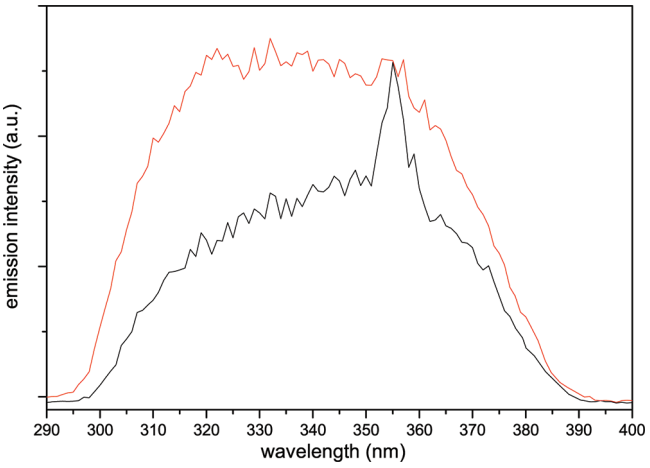

Figure 8. Fluorescence spectra measured in a quartz cuvette containing pure liquid pyridine (black trace) and a 5:1 mixture of pyridine and acetic acid (red trace).

8 GPa. A comparison between the fluorescence spectra measured at ambient pressure in the liquid and at high pressure in the solid phases allows to state that the fluorescence intensity is more than 10^6 times stronger in the crystal at 4 GPa than in the liquid phase. This observation implies a dramatic effect of the increased density on the electronic states of pyridine.

Transitions to four excited states are reported in the absorption spectrum at wavelengths above 200 nm. The transition to S_1 ($^1B_1$), of nπ^* type, has its electronic origin at 287.6 nm and maximum around 260 nm. The transitions to S_2 ($^1B_2$) and S_4 ($^1A_1$), of $\pi\pi^*$ character, have their maxima at about 250 and 200 nm, respectively. The transition to S_3 ($^1A_2$), of nπ^* character, with maximum located at about 230 nm, is not dipole allowed but is TP active.[24] A detailed review on the experimental and theoretical results on the low-lying singlet and triplet excited states of the pyridine molecule can be found elsewhere.[23] The fluorescence of jet-cooled and of vapor-phase pyridine[33] has been measured and revealed a fluorescence quantum yield monotonically decreasing with increasing the excitation energy (from 10^{-4} exciting at the 0−0 of S_1 to 10^{-6} exciting at the 0−0 of S_2) due to an increase in the rate of internal conversion to the ground state.[34] No emission measurement is reported for liquid or solid pyridine.

Transitions to nπ^* states are generally characterized by much smaller absorption cross sections (typically 2 orders of magnitude smaller) than transitions to $\pi\pi^*$ states because of the small overlap between the n and the π^* orbitals. The radiative lifetime of nπ^* states is then about 100 times longer than that of $\pi\pi^*$ and nonradiative processes become dominant.[35] Moreover, the rate of intersystem crossing is 2−3 orders of magnitude faster when the transition involves a singlet nπ^* and a lower $\pi\pi^*$ triplet states than in compounds lacking the nπ^* states.[36] In the specific case of pyridine, several mechanisms have been proposed to explain the enhancement of intersystem crossing and of internal conversion rate.[33] Some mono and dialkylpyridines, which are not fluorescent in the gas phase or in solutions, are reported to exhibit a weak fluorescence in acid solutions at low temperatures, with a maximum around 300 nm, originated by emission from a $\pi\pi^*$ state, which is the lowest excited state of the protonated species.[40] Anyway, no such fluorescence was observed for pyridine in the same conditions. Since we succeded in detecting a very weak emission from liquid pyridine at ambient conditions, we compared such emission with that of a mixture of pyridine and acetic acid in a 5:1 ratio. As can be seen in Figure 8, the effect of acidity is indeed an enhancement of emission intensity, particularly in the blue region of the spectrum.

The strong intensification of the emission in the crystal phases is clearly connected with the changes in the structural arrangement and with the related effects on the electronic structure. Both crystal structures of phases I[16] and II[17] of pyridine allow several inequivalent CH···N intermolecular interactions with distances shorter than 3 Å at 1 GPa. In phase II each molecule takes part in four CH···N contacts, two of them involving the N atom and the two others involving the H atom bonded to the α C atoms. In phase I some of the CH···N contacts are replaced by CH···π contacts, but the two crystal structures are very similar to each other, differing in the orientations of similar layers of pyridine molecules. The involvement of the N atom in two H bonds, similarly to the effect of acidity, likely lowers the energy of the N non bonding orbital, determining a blue shift of the nπ^* state. The electronic structure of pyridine is thus strongly perturbed in the crystal phases, and an inversion of the energies of the nπ^* and $\pi\pi^*$ states may likely occur. We cannot have a proof to this hypothesis by analysis of the excitation profiles, due to the too low signal intensity in the spectral region of the three lowest energy transitions. Anyway, inspection of the emission peak frequencies (Figure 5) reveals that there is a clear blue shift for the three high-frequency bands in going from the liquid to the solid phases, which is particularly pronounced (about 400 cm^{-1}) for the highest frequency peak, likely corresponding to the pure exciton band of the $S_1 \rightarrow S_0$ transition. This blue shift may actually be ascribed to the frequency difference between the exciton emission from the $^1B_2$ ($\pi\pi^*$) state in the solid and the electronic origin of the $^1B_1$ (nπ^*) state in the liquid phase. The actual observation of a blue shift is even more remarkable considering the usual red shift observed for the lowest electronic transitions on increasing pressure.[6] In addition, in the particular case of the pyridine crystal, where H bonding has a similar effect as acidity on the electronic structure, we find a support to the presence of a red shift in calculations comparing electronic transitions in pyridine and in the pyridinium ion.[37] Indeed, some examples of emission intensity enhancement in heterocyclic aromatics following crystallization or compression in interacting solvents are reported[38] and explained with a change in character of the lowest excited state from nπ^* to $\pi\pi^*$.

The fluorescence spectra have been decomposed into four bands. The lowest frequency one, showing a different intensity behavior with pressure (see Figure 4), has been assigned to excimer emission. The critical dependence of the fluorescence signal on the alignment conditions prevents a quantitative comparison of the absolute emission intensity among the different spectra. Nevertheless, comparing the data from the experiment on the not-annealed phase II sample, it is qualitatively possible to see that the intensity of the blue part of the spectrum reaches its maximum at about 6 GPa and slightly decreases at higher pressures, while the intensity of the lowest frequency peak monotonically increases with pressure upon compression and decreases only above 12 GPa. Following the explanation for fluorescence appearance in the solid state outlined above, the peak at 308 nm must be due to emission from the lowest singlet excited states of condensed pyridine having $\pi\pi^*$ character. The two peaks shifted by about 1600 and 3200 cm^{-1} to the red of the highest frequency band have a very similar pressure and intensity

behavior and are likely to be assigned to a vibronic structure of the emission from the same state. This structure is likely built on the ground state totally symmetric vibration at 1590 cm^{-1} (ν_4 mode).[39] The band at 365 nm, lying at about 5000 cm^{-1} to the red of the 308 nm band, and with an intensity that monotonically increases with compression, has been ascribed to emission from a pyridine excimer, as also suggested for mono- and dialkylpiridines in acid solutions at 77 K.[40] Excimer emission is reported for several aromatic molecular crystals at high pressures, and the role of the crystal structure and of structural defects in excimer formation has been studied in detail.[28] Crystals have been classified as type B or type A depending whether excimer formation is allowed or not allowed by the crystal structure, in the latter case being able to form only at crystal defects.[32] The crystal structures of pyridine suggest that no structural excimer can be formed in the bulk. Favorable contacts for excimer formation are indeed prevented by the hydrogen bond network, which stabilizes both crystal structures.[15] The stacked conformations typical of excimers of aromatic molecules are only allowed at crystal defects. Indeed, the intensity of the 365 nm band increases in all the situation where the number of defects is supposed to increase.

The intensification of fluorescence in the blue region of the emission spectrum has been related to the inversion of the $n\pi^*$ and $\pi\pi^*$ governed by the H-bonding interactions. This picture is confirmed by the observation that in the glassy form, where the ordered network of H-bonded molecules is lacking, the fluorescence intensity is strongly reduced, particularly in the blue region. The absolute intensity of the excimer band is much lower than in the crystal but its relative intensity is larger. Also, the relative intensity of the excimer band is much larger in the pure liquid than in all the cases where the monomer emission is induced through interaction of the N lone pair with an H atom, as in the acid solution (Figure 8) and in the crystal phases. In the liquid[41] and in the gas phase[42,43] there are several dimeric structures in the ground state, characterized by similar energies, the most stable being a T-shape configuration held toghether by a CH$\cdots\pi$ and a CH$\cdots$N interactions, and two different antiparallel arrangements, one directly stacked and the other parallelly displaced.

Excimer formation at crystal defects is also in agreement with the scarse reactivity of pyridine at high pressure.[15] In fact, pressure-induced reactivity in benzene crystals has been demonstrated to be related to the formation of dimeric structures[14] with a similar geometry as those formed in the excited state (excimers) and triggering the reaction at lower pressures.[21] These observations strongly suggest that pressure brings the system in a ground-state conformation close to the excimer structure in the excited state potential energy surface.[10] A limited reactivity, only occurring at crystal defects, has also been found in crystalline indole, where excimer formation is not allowed by the crystal structure.[11]

In our previous work[15] we found that laser light at 457 nm triggered the reaction at a pressure lower by a factor of 3 with respect to the purely pressure induced process, whereas light at 514 nm had no effect on the reactivity. Our TP excitation profiles indeed show that the 457-nm line is on the absorption edge of the S_4 state, whereas the 514-nm line is in a wavelength range where TP absorption is below our sensitivity. Therefore, excitation at 457 nm is much more efficient at creating excited molecules that after a fast decay to lower excited states give rise to the formation of the excimers. This is likely the triggering step for the amorphization reaction, as observed in crystalline benzene.[10] Anyway, in benzene the reaction propagates through the bulk of the crystal during decompression, when an extra volume is available for the formation of the saturated product. In pyridine the reaction nucleates in a limited number of sites upon compression and does not propagate upon decompression.[15] The number of reaction seeds is related to the amount of excimeric species, which can only form at crystal defects. The lack of reactivity in the glass form is also consistent because, even if the relative intensity of the excimer band is larger than in the crystal phases, the absolute intensity is much weaker as can be seen in Figure 4, indicating the existence of few potential reaction seeds.

5. CONCLUSIONS

In this work we have been able to detect, for the first time to our knowledge, fluorescence emission from condensed phases of pyridine. TP excited fluorescence and TP excitation profiles in the spectral range 420−580 nm have been measured in crystal phases I and II and in the glassy form, i.e., all the phases encountered compressing pyridine at room temperature below the amorphization reaction threshold. Samples with different compression, annealing, and irradiation histories have been monitored, and the role of structural defects in the emission properties has been evidenced.

The emission intensity rapidly increases with pressure in the crystalline phases, being at 3 GPa about 6 orders of magnitude larger than in the liquid. This intensification is explained with the inversion of the lowest $n\pi^*$ ($^1B_1$) and $\pi\pi^*$ ($^1B_2$) excited states, due to the large amount of strong CH$\cdots$N interactions building up in both crystal phases. The unique role of pressure in enhancing these interactions is evidenced by the fact that the pressure-induced fluorescence is orders of magnitude larger than the fluorescence observed by acidifying pyridine with acetic acid in 5:1 ratio. The fluorescence quantum yield increases up to about 10 GPa and slightly decreases above this pressure.

The low-frequency region of the fluorescence spectrum, consisting of a band displaced by about 5000 cm^{-1} from the exciton band, is ascribed to excimer emission. The crystal structure of both phases I and II does not allow the formation of structural excimers in a stacked geometry as instead observed in benzene crystals.[10] Excimers can thus most likely form at the structural defects. This is consistent with the not reversible and poorly reproducible, from one experiment to the other, pressure dependence of the excimer band intensity, reflecting the formation of crystal defects along the pressure cycles. Excimer formation allowed only at crystal defects is also perfectly consistent with the observation of a scarce and not reproducible from one sample to the other, reactivity in the pressure-induced amorphization.[15]

TP excitation profiles are very weak in the range of excitation to the S_1, S_2, and S_3 states, whereas we can clearly detect the absorption edge of the $S_0 \rightarrow S_4$ transition. The lowering of the reaction threshold pressure by TP laser excitation[15] is explained with excitation to this state. The low reaction yield and its dependence on the sample history suggest that it can be triggered only at crystal defects,[15] once more relating the high-pressure reactivity to the formation of species characterized by peculiar electronic structures able to initiate and propagate the reaction.

AUTHOR INFORMATION

Corresponding Author

*Phone: +390554572503. Fax: +390554572451. E-mail: margherita@lens.unifi.it.

■ ACKNOWLEDGMENT

Supported by the European Union under Contract LASERLAB EUROPE 228334 and by the Italian Ministero dell'Istruzione, dell'Università e della Ricerca (MIUR). We gratefully acknowledge constructive discussion with Prof. P. Foggi and Prof. P. R. Salvi.

■ REFERENCES

(1) Schettino, V.; Bini, R.; Ceppatelli, M.; Ciabini, L.; Citroni, M. *Adv. Chem. Phys.* **2005**, *131*, 105–242.
(2) Citroni, M.; Ceppatelli, M.; Bini, R.; Schettino, V. *Science* **2002**, *295*, 2058–2060.
(3) Chelazzi, D.; Ceppatelli, M.; Santoro, M.; Bini, R.; Schettino, V. *Nat. Mater.* **2004**, *3*, 470–475.
(4) Bini, R. *Acc. Chem. Res.* **2004**, *37*, 95–101.
(5) Ceppatelli, M.; Bini, R.; Schettino, V. *Proc. Natl. Acad. Sci.* **2009**, *106*, 11454–11459.
(6) Drickamer, H. G. *Annu. Rev. Mater. Sci.* **1990**, *20*, 1–17.
(7) Drickamer, H. G.; Frank, C. W. *Electronic Transitions and the High Pressure Chemistry and Physics of Solids*; Chapman and Hall: London, 1973.
(8) Dreger, Z. A.; Yang, G.; White, G. O.; Li, Y.; Drickamer, H. G. *J. Phys. Chem. A* **1997**, *101*, 9511–9519.
(9) Dreger, Z. A.; Balasubramaniam, E.; Gupta, Y. M.; Joly, A. G. *J. Phys. Chem. A* **2009**, *113*, 1489–1496.
(10) Citroni, M.; Bini, R.; Foggi, P.; Schettino, V. *Proc. Natl. Acad. Sci.* **2008**, *105*, 7658–7663.
(11) Citroni, M.; Costantini, B.; Bini, R.; Schettino, V. *J. Phys. Chem. B.* **2009**, *113*, 13526–13535.
(12) Jackson, B. R.; Trout, C. C.; Badding, J. V. *Chem. Mater.* **2003**, *15*, 1820–1824.
(13) Wen, X. D.; Hoffmann, R.; Ashcroft, N. W. *J. Am. Chem. Soc.* **2011**, *133*, 9023–9035.
(14) Ciabini, L.; Santoro, M.; Gorelli, F. A.; Bini, R.; Schettino, V.; Raugei, S. *Nat. Mat.* **2007**, *6*, 39–43.
(15) Fanetti, S.; Citroni, M.; Bini, R. *J. Chem. Phys.* **2011**, *134*, 204504 1–9.
(16) Podsiadlo, M.; Jakobek, K.; Katrusiak, A. *Cryst. Eng. Commun.* **2010**, *12*, 2561–2567.
(17) Crawford, S.; Kirchner, M. T.; Blaser, D.; Boese, R.; David, W. I. F.; Dawson, A.; Gehrke, A.; Ibberson, R. M.; Marshall, W. G.; Parsons, S.; Yamamuro, O. *Angew. Chem., Intl. Ed.* **2009**, *48*, 755–757.
(18) Ceppatelli, M.; Santoro, M.; Bini, R.; Schettino, V. *J. Chem. Phys.* **2003**, *118*, 1499–1506.
(19) Pruzan, P.; Chervin, J. C.; Forgerit, J. P. *J. Chem. Phys.* **1992**, *96*, 761–767.
(20) Zhuravlev, K. K.; Traikov, K.; Dong, Z.; Xie, S.; Song, Y.; Liu, Z. *Phys. Rev. B* **2010**, *82*, 064116.
(21) Ciabini, L.; Santoro, M.; Bini, R.; Schettino, V. *Phys. Rev. Lett.* **2002**, *88*, 085505 1–4.
(22) Santoro, M.; Ceppatelli, M.; Bini, R.; Schettino, V. *J. Chem. Phys.* **2003**, *118*, 8321–8325.
(23) Cai, Z.; Reimers, J. R. *J. Phys. Chem. A* **2000**, *104*, 8389–8408.
(24) Salvi, P. R.; Foggi, P.; Bini, R.; Castellucci, E. *Chem. Phys. Lett.* **1987**, *141*, 417–422.
(25) Bini, R.; Ballerini, R.; Pratesi, G.; Jodl, H. J. *Rev. Sci. Instrum.* **1997**, *68*, 3154–3160.
(26) Yamazaki, I.; Baba, H. *J. Chem. Phys.* **1977**, *66*, 5826–5827.
(27) Wojdyr, M. *J. Appl. Crystallogr.* **2010**, *43*, 1126–1128.
(28) Dreger, Z. A.; Lucas, H.; Gupta, Y. M. *J. Phys. Chem. B* **2003**, *107*, 9268–9274.
(29) Brillante, A.; Della Valle, R. G.; Farina, R. *Chem. Phys.* **1995**, *191*, 177–184.
(30) Jones, P. F.; Nicol, M. *J. Chem. Phys.* **1968**, *48*, 5440–5446.
(31) Offen, H. W. *J. Chem. Phys.* **1966**, *44*, 699–703.
(32) Stevens, B. *Spectrochim. Acta* **1966**, *18*, 439–448.
(33) Villa, E.; Amirav, A.; Lim, E. C. *J. Phys. Chem.* **1988**, *92*, 5393–5397.
(34) Yamazaki, I.; Sushida, K.; Baba, H. *J. Chem. Phys.* **1979**, *71*, 381–387.
(35) Valeur, B. *Molecular Fluorescence: principles and applications*; Wiley-VCH: Weinheim, 2002.
(36) El-Sayed, M. A. *Acc. Chem. Res.* **1968**, *1*, 8–16.
(37) Yoshida, Z.; Kobayashi, T. *Theor. Chim. Acta* **1971**, *20*, 216–226.
(38) Drickamer, H. G. *Annu. Rev. Phys. Chem.* **1982**, *33*, 25–47.
(39) Klots, T. D. *Spectrochim. Acta* **1998**, *A 54*, 1481–1498.
(40) Handa, T.; Utena, Y.; Yajima, H.; Ishii, T.; Morita, H. *J. Phys. Chem.* **1986**, *90*, 2589–2596.
(41) Baker, C. M.; Grant, G. H. *J. Chem. Theor. Comput.* **2007**, *3*, 530–548.
(42) Mishra, B. K.; Sathyamurthy, N. *J. Phys. Chem. A* **2005**, *109*, 6–8.
(43) Piacenza, M.; Grimme, S. *Chem. Phys. Chem.* **2005**, *6*, 1554–1558.